IV Escola de Primavera de Transição e Turbulência
Universidade Federal do Rio Grande do Sul
Pontifícia Universidade Católica do Rio Grande do Sul
Porto Alegre, RS, 27 de setembro a 1° de outubro de 2004

DEVELOPMENT OF A COMPUTATIONAL CODE FOR STUDYING COMPRESSIBLE SHEAR LAYER FLOW INSTABILITIES

Ricardo A. Coppola Germanos
USP - Universidade de São Paulo
Escola de Engenharia de São Carlos - Departamento de Engenharia Aeronáutica
Av. Trabalhador São Carlense, 400 - SP - 13566-590, Brazil
gercop@sc.usp.br

Marcello A. Faraco de Medeiros
USP - Universidade de São Paulo
Escola de Engenharia de São Carlos - Departamento de Engenharia Aeronáutica
Av. Trabalhador São Carlense, 400 - SP - 13566-590, Brazil
marcello@sc.usp.br

Leandro F. de Souza
USP - Universidade de São Paulo
Instituto de Ciências Matemáticas e de Computação – Departamento de Ciências de Computação e Estatística
Av. Trabalhador São Carlense, 400 - SP - 13560-970, Brazil
lefraso@icmc.usp.br

Abstract. *Code accuracy is a very important aspect of Direct Numerical Simulation. Verification of the accuracy of such codes is often performed by comparison with analytical solutions of selected linear problems. An example of the procedure is given in the paper. In order to verify the computational code the standing acoustic waves problem was adopted. This problem can be linearized assuming that the amplitude of the acoustic waves is very small. However, in many instances the linear analysis becomes a very complicated task, in particular when viscous and compressible effects are considered. This test gives an estimation of the numerical error. An application of the method is given a free-shear layer flow.*

keywords: *Numerical methods, Hydrodynamic instability, Compressible free shear layer, Transition.*

1. Introduction

In studies of flows by Direct Numerical Simulation (DNS), the researcher should simulate all scales and frequencies properly. There are many sources of numerical errors, and, if these errors are not minimized, the results obtained could not reproduce the physics of the problem. Thus code testing is of paramount importance in this field.

Transition and turbulent flows possess wide range of space and time scales. Therefore, these kind of flows requires high accuracy in the numeric solution. This requirement of accuracy can be achieve by the use of spectral methods (Canuto et al., 1987). The use of this schemes is restricted to flows in simple domains and simple boundary conditions. In order to overcome these difficulties an alternative numeric representations can be used, as the Finite Differences Schemes and the Finite Volume Schemes. The Finite Differences Schemes is justified by the possibility of the use of more general boundary conditions, although the schemes with high order of accuracy also restricted to the problem with simple domains. The advantage of these schemes in relation to Finite Volume Schemes is that high order approximations can be used. The Finite Volume Schemes has advantages in working with complex domains and also with complex boundary conditions. The Finite difference schemes may be classified as explicit or implicit. According to Mahesh, 1998, implicit schemes are significantly more accurate for the small scales than explicit schemes with the same stencil width. The implicit schemes are extremely attractive when explicit time advancement schemes are used.

The accuracy of a code can be performed by comparison with analytical. In this study a solution of the standing acoustic wave problem with small amplitude was adopted as case test. A very good theory of acoustic waves can be found in Morse and Ingard, 1968. After the comparison of numerical results with the analytical solution, the compressible free shear layer problem was simulated. Sandham and Reynolds, 1989, Lessen et al., 1966 and Blumen, 1970 presents theoretical results with this problem.

In order to solve the spatial derivatives, the implicit schemes also called compact schemes was adopted. The finite difference approximation to the derivative of the function is expressed as a linear combination of the given function values on a set of nodes. In compact finite difference schemes the value of f_i' possess a dependence with all the values of nodes.

Lele, 1992 emphasizes the importance of using methods of high order and proposes a 3^{rd} order approximation

at the boundaries and a 4^{th} order approximation for points near the boundaries. In this work a different discretization of the boundary and near boundary points was adopted according to Souza et al., 2002.

The boundary condition adopted in the x direction was periodic. In the y direction is not possible to use a periodic boundary conditions and thus the Neumann or free-slip boundary conditions was used according Medeiros et al., 2000 and Souza, 2003. Thompson, 1987 presents non-reflecting boundary conditions. The idea of these boundary conditions is to consider the characteristic form of the Euler equation at the boundary. Another possibility is to use an exponential decay, except that this method is only rigorously correct in the linear regime. In the current work the free-slip boundary condition in the y direction was adopted. This boundary condition should produce accurate results for a sufficient large distance from the shear layer.

To solve the temporal derivatives a another method was adopted. In agreement with Williamson, 1980, the time-advance is obtained by a high order Runge-Kutta schemes. This schemes is conditionally stable. In this study is interesting to capture the transient effects. In order to simulate these phenomena appropriately is necessary to use a small time increments in the numeric simulation to assure that the criterion of stability was satisfied. Therefore the restrictions of stability are only two: that due to convection and due to the diffusion. This same schemes is used by Kloker et al., 1993.

The organization of the paper is as follows. Section 2 presents the formulation adopted in the current work. The details of the numerical method is described in the section 3. Initial and boundary condition are discussed and the compact schemes and Runge-Kutta are described with more details. Section 4 presents analysis of the verification of computational code and shows a numerical simulation of the free shear layer phenomena. The last section presents the conclusion of this work.

2. Formulation

In this study, the governing equations are the compressible, isentropic, bi-dimensional Navier-Stokes equations (Sandham and Reynolds, 1991; Eibler and Bestek, 1996). They consist of the momentum equations for the velocity component (u,v) in the streamwise direction (x) and normal direction (y):

$$\frac{\partial \rho u}{\partial t} = -\frac{\partial \rho u^2}{\partial x} - \frac{\partial \rho uv}{\partial y} - \frac{\partial p}{\partial x} + \frac{1}{Re}\left(\frac{4}{3}\frac{\partial^2 u}{\partial x^2} + \frac{\partial^2 u}{\partial y^2} + \frac{1}{3}\frac{\partial^2 v}{\partial x \partial y}\right), \tag{1}$$

$$\frac{\partial \rho v}{\partial t} = -\frac{\partial \rho v^2}{\partial y} - \frac{\partial \rho uv}{\partial x} - \frac{\partial p}{\partial y} + \frac{1}{Re}\left(\frac{4}{3}\frac{\partial^2 v}{\partial y^2} + \frac{\partial^2 v}{\partial x^2} + \frac{1}{3}\frac{\partial^2 u}{\partial x \partial y}\right), \tag{2}$$

and the continuity equation:

$$\frac{\partial \rho}{\partial t} = -\frac{\partial \rho u}{\partial x} - \frac{\partial \rho v}{\partial y}, \tag{3}$$

where x and y is the Cartesian coordinates and t is the time. The primitive variables (u, v, ρ and p) are the velocity component in the x and y direction, the density and the pressure, respectively.

These equations were defined with the following non-dimensionalization scheme:

$$u_i = \frac{u_i^*}{c^*}, \quad \rho = \frac{\rho^*}{\rho_0^*}, \quad p = \frac{p^*}{\rho_0^* \, c^{*2}}, \quad t = \frac{t^* c^*}{\delta_{\omega_0}^*}, \quad x_i = \frac{x_i^*}{\delta_{\omega_0}^*}, \tag{4}$$

where c^* is the sound speed and ρ_0^* is the mean flow density, $\delta_{\omega_0}^*$ is the vorticity thickness of the initial velocity given by:

$$\delta_{\omega_0}^* = \frac{U_1^* - U_2^*}{|d\bar{u_0}^*/dy^*|_{max}}, \tag{5}$$

where the subscript 1 e 2 refers to the upper ($y > 0$) and lower ($y < 0$) free stream, respectively. The Reynolds number of the flow is defined by:

$$Re = \frac{\rho_0^* \, c^* \, \delta_{\omega_0}^*}{\mu^*}, \tag{6}$$

where μ^* is the dynamic viscosity.

In the actual stage, an isentropic flow hypothesis was adopted (Sullivan, 1981). Therefore, the equation of the perfect gases combined with to the equation of energy can be written in the following way:

$$p = \left(\frac{p_0^*}{\rho_0^* \, c^{*2}}\right) \rho^\gamma, \tag{7}$$

where p_0^* is the mean flow pressure and $\gamma = c_p/c_v$ is the relation of the specific heat.

In the next section is presented the numerical methods and the boundary and initial conditions adopted in this work. Details about compact and Runge-Kutta schemes are described bellow.

3. Numerical Method

This section presents the numerical method adopted for a time-developing free shear layer problem. In order to solve the spatial derivatives, 6^{th} order compact finite difference schemes was adopted. A periodic condition in the x direction was setted. At the boundaries in the y direction a Neumann condition was adopted. The objective of this work is to analyze the variation of the amplification rate of the disturbance. In the present work the variables was decomposed in two parts: temporary mean and small disturbance. This way the primitive variables can be written in the following way:

$$u(x,y,t) = \bar{u_0} + u', \tag{8}$$
$$v(x,y,t) = \bar{v_0} + v', \tag{9}$$
$$\rho(x,y,t) = \bar{\rho_0} + \rho'. \tag{10}$$

The mean flow is invariant in the longitudinal direction and that to normal component of mean velocity is null. In other words, the mean flow is locally parallel. It was also assumed that the mean flow is steady along the time and that the pressure gradients are negligible.

Tests with standing acoustic waves was carry out to verify the numerical code. The accuracy of this code was performed by comparison with analytical solution. Finding analytical solutions of the Navier-Stokes equations is not easy due to non-linearity. These difficulties may be overcome when small amplitudes disturbance are used. Taking this into account, the equations can be linearized to obtain an analytical solution. This assumption is consistent if the fluctuations are very small. Therefore, with an analytical solution it was possible to evaluate the order of the numerical method. The analytical solutions of the standing acoustic waves adopted in this case test was:

$$\begin{aligned} u' &= \widehat{u}_1 \exp(i\alpha x + i\beta y - \omega_1 t) + \widehat{u}_2 \exp(i\alpha x + i\beta y - \omega_2 t), \\ v' &= \widehat{v}_1 \exp(i\alpha x + i\beta y - \omega_1 t) + \widehat{v}_2 \exp(i\alpha x + i\beta y - \omega_2 t), \\ \rho' &= \widehat{\rho}_1 \exp(i\alpha x + i\beta y - \omega_1 t) + \widehat{\rho}_2 \exp(i\alpha x + i\beta y - \omega_2 t), \end{aligned}$$

where

$$\widehat{u}_1 = \widehat{u}_2 = 1, \tag{11}$$

$$\widehat{v}_1 = \widehat{v}_2 = \frac{\beta}{\alpha}, \tag{12}$$

$$\widehat{\rho}_1 = \frac{3i\rho_0^{*^2}\,(\alpha + \widehat{v}_1\beta)}{2\mu^*\,(\alpha^2+\beta^2) + i\sqrt{(\alpha^2+\beta^2)\,(-4\mu^{*2}(\alpha^2+\beta^2) + 9\rho_0^{*2}c^{*2})}}, \tag{13}$$

$$\widehat{\rho}_2 = \frac{3i\rho_0^{*^2}\,(\alpha + \widehat{v}_2\beta)}{2\mu^*\,(\alpha^2+\beta^2) - i\sqrt{(\alpha^2+\beta^2)\,(-4\mu^{*2}(\alpha^2+\beta^2) + 9\rho_0^{*2}c^{*2})}}, \tag{14}$$

$$w_1 = \frac{2\mu^*(\alpha^2+\beta^2) + i\sqrt{(\beta^2+\alpha^2)\,(-4\mu^{*2}(\alpha^2+\beta^2) + 9\rho_0^{*2}c^{*2})}}{3\rho_0^*}, \tag{15}$$

$$w_2 = \frac{2\mu^*(\alpha^2+\beta^2) - i\sqrt{(\beta^2+\alpha^2)\,(-4\mu^{*2}(\alpha^2+\beta^2) + 9\rho_0^{*2}c^{*2})}}{3\rho_0^*}. \tag{16}$$

The initial condition adopted for the numerical simulations was extracted of this analytical solution. In the section 4, more details of test case is described.

These tests are the first stage for the free shear layer simulation. This problem develops from specified initial conditions (Fortuné, 2000). Hyperbolic tangent mean profile was used:

$$\bar{u_0} = \left(\frac{U_1^* - U_2^*}{2}\right)\tanh(2y), \tag{17}$$

where U_1^* and U_2^* are the upper ($y > 0$) and the lower ($y < 0$) free stream. Along with the velocity profile the disturbances were defined as:

$$u' = \frac{2\sigma y}{(\alpha_1\alpha_2)}\left[A_1\sin(\alpha_1 x)\alpha_2 + A_2\sin(\alpha_2 x)\alpha_1\right]\exp(-\sigma y^2), \tag{18}$$

$$v' = \left[A_1\sin(\alpha_1 x) + A_2\sin(\alpha_2 x)\right]\exp(-\sigma y^2), \tag{19}$$

$$\rho' = 0, \tag{20}$$

where A is the amplitude, α is the wavenumber and σ is the spread of the disturbance in the y direction. The subscript 1 refers to the dominant mode and subscript 2 refers to the subharmonic excitation. Uniform density is assumed for the initial mean flow ($\rho = 1.2256$), so the mean pressure is obtained by the equation 7.

Bellow the discretization used in the streamwise and normal direction are present. The letter i, j represents the grid position in x and y direction, which varies from 0 to N, M respectively. In the x direction the 6^{th} order implicit (compact) derivatives for $0 < i < N$ as follows:

$$\begin{bmatrix} 3 & 1 & & & & & 1 \\ 1 & 3 & 1 & & & & \\ & \ddots & \ddots & \ddots & & & \\ & & 1 & 3 & 1 & & \\ & & & \ddots & \ddots & \ddots & \\ & & & & 1 & 3 & 1 \\ 1 & & & & & 1 & 3 \end{bmatrix} \begin{bmatrix} f'_{0,j} \\ f'_{1,j} \\ \vdots \\ f'_{i,j} \\ \vdots \\ f'_{N-1,j} \\ f'_{N,j} \end{bmatrix} = \begin{bmatrix} \frac{1}{12dx}(f_{N-1,j} + 28f_{N,j} - 28f_{1,j} - f_{2,j}) \\ \frac{1}{12dx}(f_{N,j} + 28f_{0,j} - 28f_{2,j} - f_{3,j}) \\ \vdots \\ \frac{1}{12dx}(f_{i+2,j} + 28f_{i+1,j} - 28f_{i-1,j} - f_{i-2,j}) \\ \vdots \\ \frac{1}{12dx}(f_{N-3,j} + 28f_{N-2,j} - 28f_{N,j} - f_{0,j}) \\ \frac{1}{12dx}(f_{N-2,j} + 28f_{N-1,j} - 28f_{0,j} - f_{1,j}) \end{bmatrix}.$$

The schemes described bellow was used by Souza et al., 2002. At the boundaries a 5^{th} order asymmetric approximation was proposed, whereas for points near the boundaries a 6^{th} order asymmetric approximation was used. For the interior points, a 6^{th} order symmetric approximation was adopted. This schemes was modified to work with the free-slip boundary condition. The 6^{th} order implicit (compact) derivatives with free-slip boundary condition for $0 < i < M$ adopted was:

$$\begin{bmatrix} 1 & & & & & & \\ 1 & 6 & 2 & & & & \\ & \ddots & \ddots & \ddots & & & \\ & & 1 & 3 & 1 & & \\ & & & \ddots & \ddots & \ddots & \\ & & & & 2 & 6 & 1 \\ & & & & & & 1 \end{bmatrix} \begin{bmatrix} f'_{i,0} \\ f'_{i,1} \\ \vdots \\ f'_{i,j} \\ \vdots \\ f'_{i,M-1} \\ f'_{i,M} \end{bmatrix} =$$

$$\begin{bmatrix} 0.0 \\ \frac{1}{120dy}(-406f_{i,0} - 300f_{i,1} + 760f_{i,2} - 80f_{i,3} + 30f_{i,4} - 4f_{i,5}) \\ \vdots \\ \frac{1}{12dy}(f_{i,j+2} + 28f_{i,j+1} - 28f_{i,j-1} - f_{i,j-2}) \\ \vdots \\ \frac{1}{120dy}(406f_{i,M} + 300f_{i,M-1} - 760f_{i,M-2} + 80f_{i,M-3} - 30f_{i,M-4} + 4f_{i,M-5}) \\ 0.0 \end{bmatrix}.$$

Finally the 4^{th} order Runge-Kutta scheme is presented. The discretized transport equations are used to determine the values of the variables at each point of the computational domain at time $t_{n+1} = t_n + dt$. The schemes here described works in 4 steps, (Ferziger and Peric, 1997):

$$f^*_{n+\frac{1}{2}} = f_n + \frac{dt}{2} f(t_n, f_n), \tag{21}$$

$$f^{**}_{n+\frac{1}{2}} = f_n + \frac{dt}{2} f(t_{n+\frac{1}{2}}, f^*_{n+\frac{1}{2}}), \tag{22}$$

$$f^*_{n+1} = f_n + dt f(t_{n+\frac{1}{2}}, f^{**}_{k+\frac{1}{2}}), \tag{23}$$

$$f_{n+1} = f_n + \frac{dt}{6}[f(t_n, f_n) + 2f(t_{n+\frac{1}{2}}, f^*_{n+\frac{1}{2}}) + 2f(t_{n+\frac{1}{2}}, f^{**}_{n+\frac{1}{2}}) + f(t_{n+1}, f^*_{n+1})]. \tag{24}$$

The first two steps, Eq. 21 and 22 use a formulation of Euler "predictor" explicit and a formulation of Euler "corrector" implicit for the same time $t + dt/2$. The following step (23) is a "predictor" based on the rule of the medium point for the whole step $(t + dt)$ and the last (24), "corrector" is based on Simpson's rule. The combination of these steps results in a 4^{th} order accuracy algorithm.

The next section presents results of the test case with standing wave problem and results obtained with the free shear layer problem.

4. Numerical Results

This section presents the results obtained with the numerical code. First, for verification of the method, tests were carry out with stating acoustic wave problem and the results were compared with linear analytical solution. After the free shear layer problem was simulated with one and two modes.

4.1. Analysis of the Numerical Error

This section presents an analysis of the spatial discretization error. The standing acoustic wave problem was simulated. The analytical solution was obtained linearizing the adopted equations. Therefore the truncation error of the spatial approximations was carried out analyzing the results obtained with mesh with different sizes. In the numeric solution there are many source of errors: the modeling error, due to the linearity of the equations; the discretization error introduced by the time advance algorithm (temporal error) and the spatial discretization error. The temporal and spatial discretization error includes the round-off and truncation error. In order to verify the order of the spatial approximations, one have to assure that the spatial round-off error, together with the other errors are negligible.

In order to obtain the analytical solutions it is necessary to linearize the involved equations. Thus can give error due to the non-linearity behavior of the Navier-Stokes equations. These equations implemented in the numerical code includes the non-linear terms. During the simulations we had to assure that the magnitude of these non linear terms was very small. To estimate the modeling error, simulations with the linear and non-linear equations were carried out and the difference between the two solutions for several wave amplitudes were calculated. Figure 1 shows that the modeling error increases with the wave amplitude. It can be concluded that this error becomes negligible for amplitudes smaller than 10^{-8}. Similar results were obtained for the density and pressure.

In this analysis it was also required to work with a time step (dt) much smaller than the distance between two consecutive points in the x direction – (dx). According with this assumption the temporal discretization error persist small in comparison with the spatial discretization error. For the tests the time step (dt) was 10^{-6}.

Finally the spatial discretization error is the combination of the round-off and truncation error. As shown in Fig. 2 the truncation error increases with the distance between two consecutive points (dx), whereas the round-off error decreases. It is difficult to estimate the values of the round-off error in relation to the truncation error, but one can estimates where each error is more significant. Figure 3 shows the sum of the round-off and truncation error called total error.

In the same way the predominance of the total error with the numeric solutions was estimated. Figure 4 shows the behavior of the maximum numerical error in function of the spatial discretization interval (dx). In order to assure that the round-off error adopted was much smaller than the truncation error, the distance between two consecutive points had values superior to 0.01.

To estimate the order of the spatial approximation schemes two different meshes were used, one with $dx = 0.1$ and the other with $dx = 0.2$. Mode details of the estimation of the order can be found in Souza, 2000. Figure 5, 6 and 7 presents the spatial approximation schemes for velocity component, density and pressure respectively.

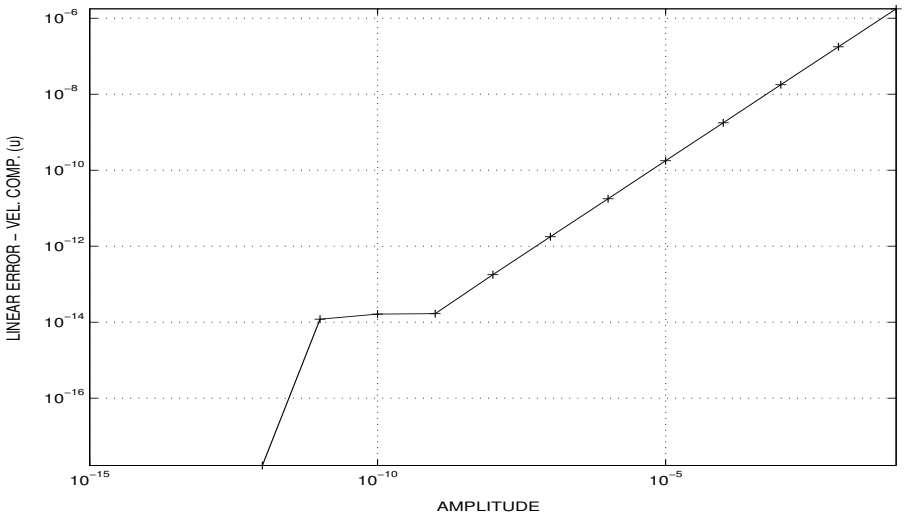

Figure 1: Modeling error due the linearity of Navier-Stokes equations

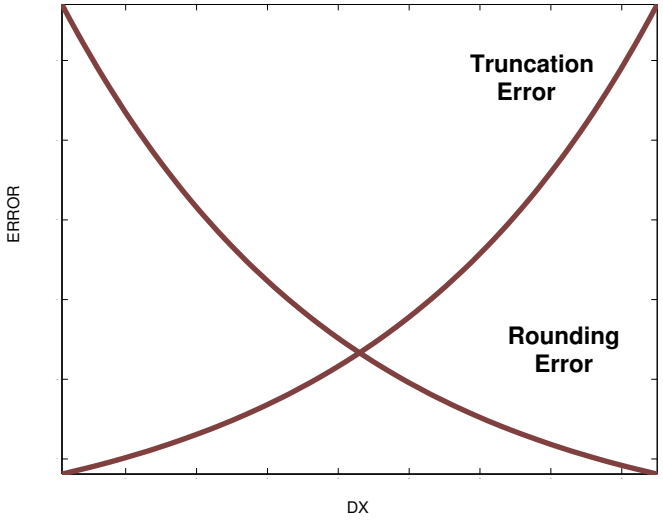

Figure 2: Theoretic round-off and Truncation Error

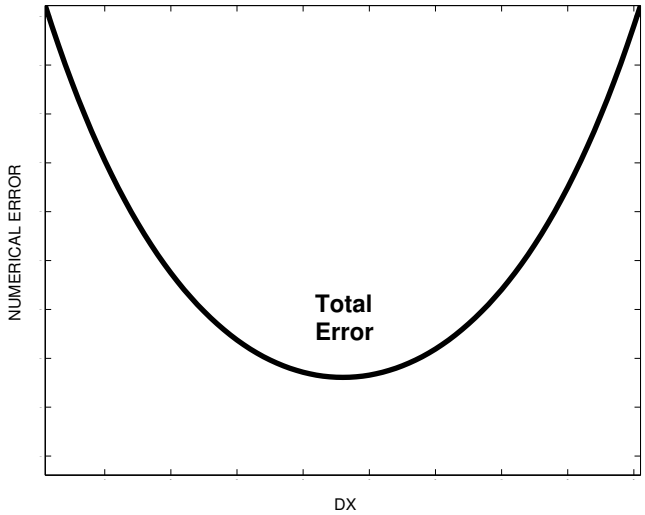

Figure 3: Theoretic Total Error (round-off Error + Truncation Error)

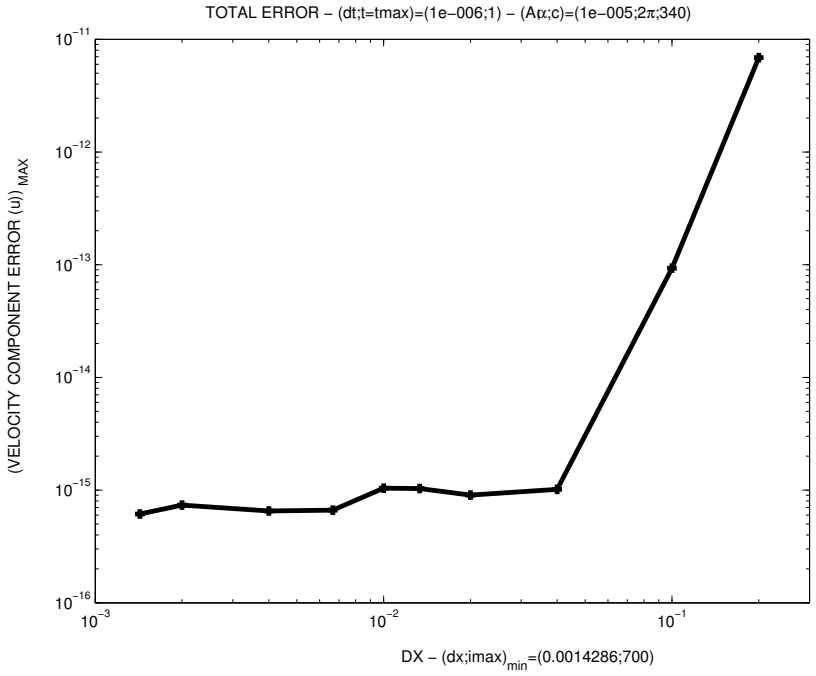

Figure 4: Numerical Total Error (round-off Error + Truncation Error)

In these figures, it can be observed that the schemes used to calculate the spatial derivatives produced results with approximately 6^{th} order of accuracy. It was not possible to estimate the order of the numerical schemes with $dx < 0.1$, due to the predominance of the round-off error.

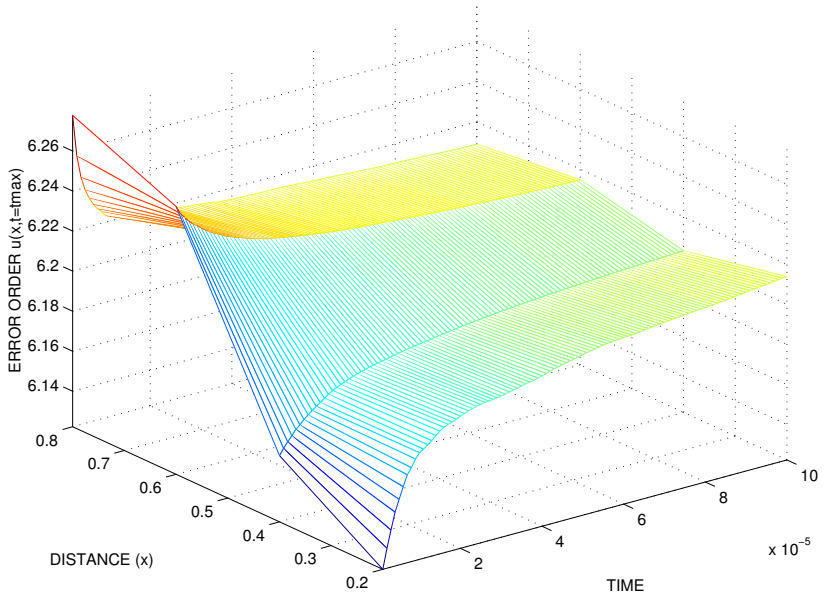

Figure 5: Truncation Error for Velocity Component u

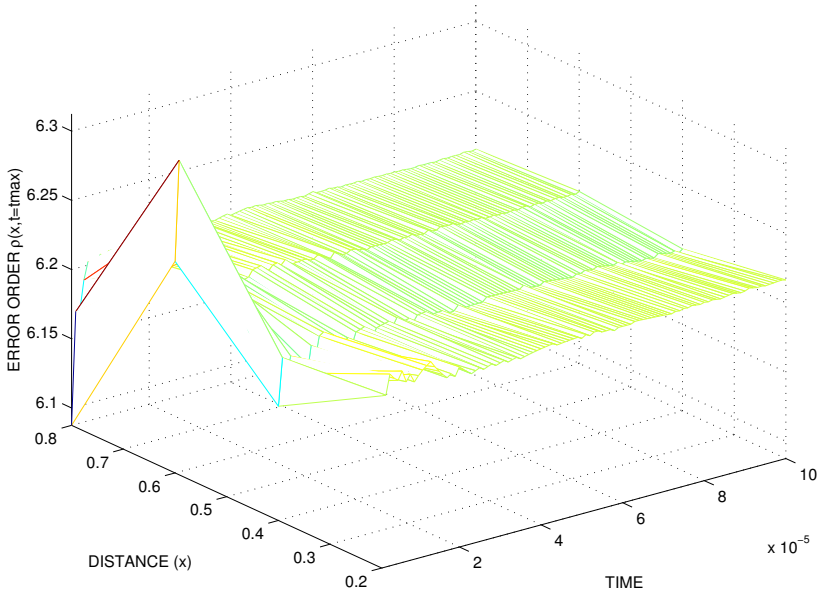

Figure 6: Truncation Error for Velocity Component ρ

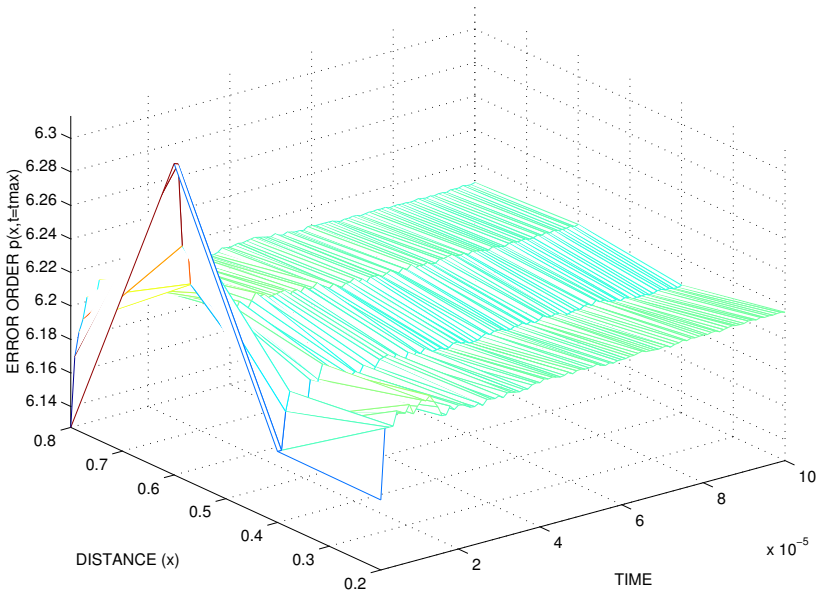

Figure 7: Truncation Error for Velocity Component p

4.2. Free Shear Layer

Here the numerical results with the free shear layer problem are presented. In the current stage of this work it was carried out the analysis of the amplification rate in linear regime. The results were compared with analytical linear result. In the non-linear regime, first, it was simulated a flow using a small disturbance of a stipulated mode. In order to reproduce the secondary instability, it were selected small disturbances composed by a dominant and a subharmonic mode.

The evolution of small disturbance in a free shear layer of the hyperbolic tangent profile was simulated. In the y direction, a free-slip boundary condition was adopted. In the x direction a periodic boundary condition was used. An important aspect to the considered in these simulations is the treatment of the vertical diffusion. This diffusion increases the width of the free shear layer during the simulation, which implies in a variation of the mean flow. Thus, there should be a variation of the amplification rate, even in the linear regime. The strategy adopted here, to avoid this diffusion, was to cancel the vertical diffusions terms.

The wavenumber of the disturbance used in the simulation was $\alpha = \pi/8 \approx 0.39$, the initial disturbance amplitude was 10^{-6}, the Reynolds number was 400, and the Mach number was 0.4. Sandham and Reynolds, 1991 shows the amplification rate for a inviscid flow at Mach number 0.4 is approximately 0.3. Figure 8 shows the numerical solution obtained in this work.

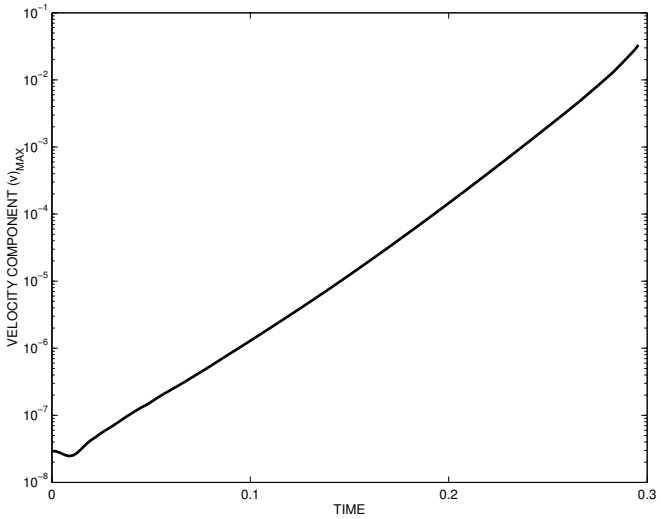

Figure 8: Amplitude Evolution

Figure 9 shows the sequence of the evolution of disturbances in time of a free shear layer flow. The boundary conditions were the same of the linear tests. The disturbance was composed by only one mode with wavenumber $\alpha = \pi/8$ .The amplitude of this mode was 10^{-3}. It can be observed that the disturbance thickness increases until the limit cycle oscillation. Figure 10 shows the evolution in time of the disturbance composed by two modes: $\alpha_1 = \pi/8$ and $\alpha_2 = \alpha_1/2 = \pi/4$ (subharmonic mode). The amplitude of the dominant mode was 10^{-3}, while the amplitude of the subharmonic mode was 10^{-4}. The secondary instability can be observed in these frames with the expected pairing of the vortices.

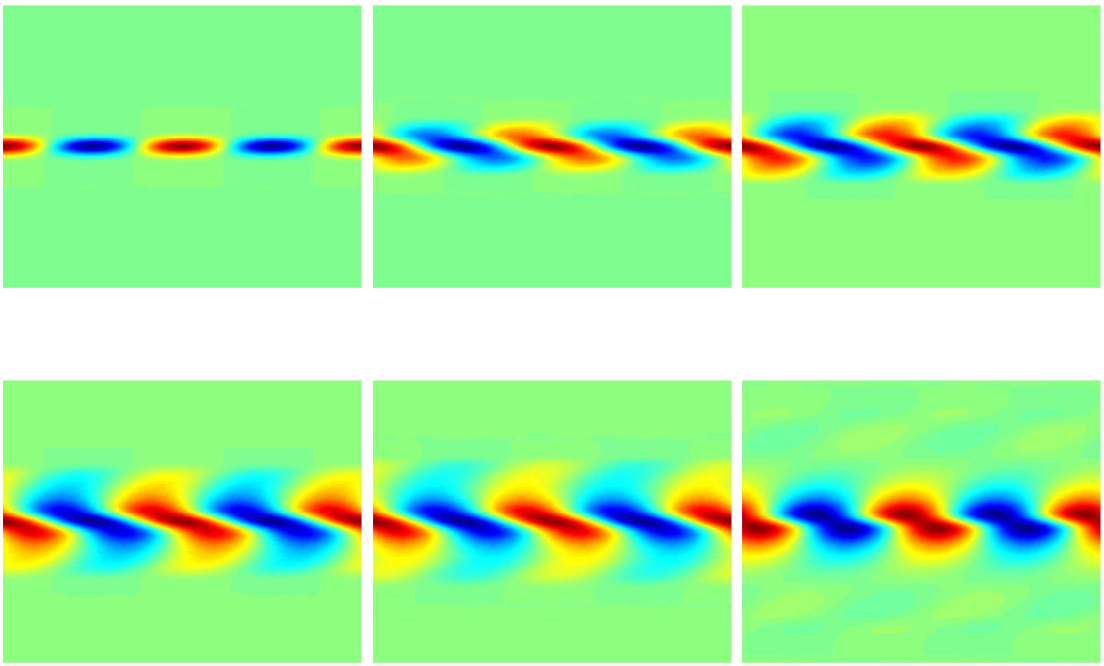

Figure 9: The linear and non-linear evolution of disturbance (v') composed of only mode.

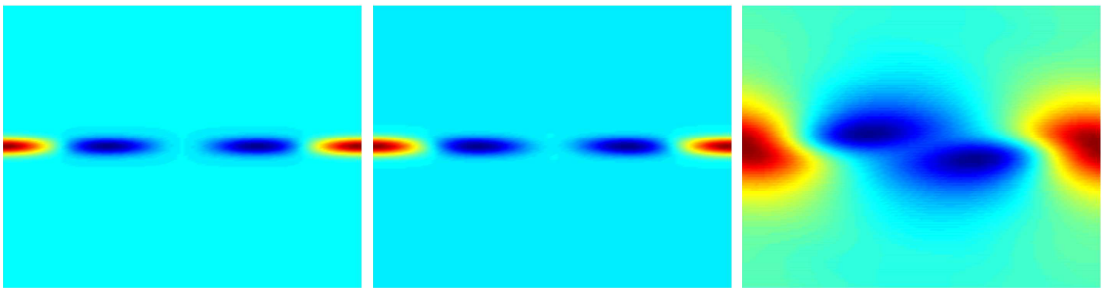

Figure 10: The linear and non-linear evolution of disturbance (v') composed of dominant mode and a subharmonic mode.

5. Conclusions

In this work numerical simulation of a standing acoustic waves was performed. The mathematical model was the Navier-Stokes equations for a isentropic one-dimensional flow. This problem was selected with the objective of estimate the order of the spatial approximations for the derivatives. The results were very good and the order obtained with this analysis was 6^{th}. This test case was very important tool for the verification of the computational code. This test was the first step of a research that aims the simulations of transitional compressible flows. The shear layer compressible flow was simulated giving some interesting results. In the linear regime was possible to obtain an good amplification rate in agreement with another works. The secondary instability also was simulated. The results for all cases with the free shear layer problem were good. Future works will present more detailed analysis of this phenomena.

6. Acknowledgments

The financial support from FAPESP (State of Sao Paulo Research Support Foundation) – Grant number 02/09256-3 is greatly acknowledged.

7. References

Blumen, W., 1970, Shear Layer instability of an inviscid compressible fluid, "Journal of Fluid Mechanics", Vol. 70, pp. 769–781.

Canuto, C., Hussaini, M. Y., Quarteroni, A., and Zang, T. A., 1987, "Spectral Methods in Fluid Dynamics".

Eibler, W. and Bestek, H., 1996, Spatial Numerical Simulations of Linear and Weakly Nolinear Wave Instabilities in Supersonic Boundary Layers, "Theoretical and Computational Fluid Dynamics", Vol. 8, pp. 219–235.

Ferziger, J. H. and Peric, M., 1997, "Computational methods for fluid dynamics".

Fortuné, V., 2000, "Étude par Simulation Numérique Directe du rayonnement acoustique de couches de mélange isothermes et anisothermes", PhD thesis, Université de Poitier.

Kloker, M., Rist, R., and Fasel, H., 1993, Outflow boundary conditions for spatial Navier-Stokes simulations of boundary layer transition, "AIAA J.", Vol. 31, pp. 620–628.

Lele, S. K., 1992, Compact finite difference schemes with spectral-like resolution, "J. Comp. Phys.", Vol. **103**, pp. 16–42.

Lessen, M., Fox, J., and Zien, H., 1966, Stability of the laminar Mixing of two Parallel Streams with respect to Supersonic Disturbances, "Journal of Fluid Mechanics", Vol. 25, pp. 737–742.

Mahesh, K., 1998, A Family of High Order Finite Difference Schemes Spectral Resolution, "J. Comp. Phys.", Vol. **145**, pp. 332–358.

Medeiros, M. A. F., Silvestrini, J. H., and and, M. T. M., 2000, Using Linear and non Linear Stability Theory for Evaluating Code Accuracy.

Morse, P. M. and Ingard, K. U., 1968, "Theoretical Acoustics", McGraw-Hill, New York.

Sandham, N. D. and Reynolds, W., 1989, Compressible Mixing Layer: Linear Theory and Direct Simulation, "AIAA Journal", Vol. 28, pp. 618–624.

Sandham, N. D. and Reynolds, W., 1991, Three-dimensional simulations of large eddies in the compressible mixing layer, "Journal of Fluids Mechanics", Vol. 224, pp. 133–158.

Souza, L. F., 2000, "Análise de algoritmos para Simulação Computational do Escoamento em uma Expansão Brusca com Controle por Sucção", PhD thesis, Pontífica Universidade Católica de Minas Gerais.

Souza, L. F., 2003, "Instabilidade Centrífuga e Transição para Turbulência em Escoamentos Laminares sobre

Superfície Côncavas", PhD thesis, Instituto Tecnológico de Aeronaútica.
Souza, L. F., Mendonça, M. T., and Medeiros, M. A. F., 2002, Assessment of Different Numerical Schemes and Grid Refinement for Hydrodynamic Stability Simulations, "ENCIT 2002", Vol. CIT02-0804.
Sullivan, D. A., 1981, Historical Review of Real-Fluid Isentropic flow Models, "J. Fluids. Eng.", Vol. 103.
Thompson, K. W., 1987, Time depedent boundary conditions for hyperbolic systems, "J. Comput. Phys.", Vol. 68, pp. 1–24.
Williamson, J. H., 1980, Low-storage Runge-Kutta Schemes, "J. Comp. Phys.", Vol. 35, pp. 48–56.

8. Copyright Notice